SCIENCE CHINA
Technological Sciences

• Article •

November 2014 Vol.57 No.11: 2153–2160
doi: 10.1007/s11431-014-5684-0

The impact of solvent and modifier on ZnO thin-film transistors fabricated by sol-gel process

DONG YinMao[1], TANG DongYan[2] & LI ChenSha[1,3*]

[1]*School of Sciences/Beijing Key Lab of Plant Resource Research and Development, Beijing Technology and Business University, Beijing 100048, China;*
[2]*School of Chemical Engineering and Technology, Harbin Institute of Technology, Harbin 150001, China;*
[3]*Department of Mechanical Engineering, Tsinghua University, Beijing 100084, China*

Received April 30, 2014; accepted July 21, 2014; published online October 15, 2014

Techniques for fabricating solution-processed zinc oxide (ZnO)-based thin-film transistors (TFTs) are feasible with solution using various routes. Here, ZnO TFTs were fabricated via sol-gel method using zinc acetate as the starting reagent with different modifiers and solvents. The ZnO thin-film semiconductors with well-controlled, preferential crystal orientation and densely packed ZnO crystals can be prepared with the optimized fabrication conditions, exhibiting excellent field-effect far exceeding those of hydrogenated amorphous silicon (a-Si:H). However, the field-effect characteristics of ZnO TFTs were different for different precursor systems which were constituted by zinc acetate, modifiers and solvents. The co-modification of acetoin and monoethanolamine for the precursor system exhibited higher extent of crystal orientation and field-effect. The maximum mobility of 7.65 $cm^2V^{-1}s^{-1}$ and current on-to-off ratio of ~$10^5 – 10^6$ have been obtained.

thin-film transistor, semiconductor, zinc oxide, sol-gel, solution-process, crystallization

Citation: Dong Y M, Tang D Y, Li C S. The impact of solvent and modifier on ZnO thin-film transistors fabricated by sol-gel process . Sci China Tech Sci, 2014, 57: 2153–2160, doi: 10.1007/s11431-014-5684-0

1 Introduction

The innovative technologies for transparent electronics have been eagerly researched and developed in the past decade. Numerous applications and designs have been developed, such as transparent conducting electrodes, light emission, sensing devices, optical wave guide devices, head-up displays in windshields of cars or planes, and transparent active-matrix displays including transparent flat-panel TVs, etc [1–4]. Being the key active device for logic integrated circuits and memories, the most prevalent transparent field-effect transistors (FETs), are made of metal-insulator-semiconductor FET based on zinc oxide (ZnO) and related oxides [4–6]. In the near future, they are most likely to substitute amorphous silicon thin-film transistors in active-matrix displays due to their excellent environmental stability, non-toxic nature, transparency and superior electronic properties (electron mobility and on/off-ratio), that are necessary to drive future display formats such as ultra-high definition and higher frame rates.

The fabrication of oxide semiconductor devices is generally based on multiple photolithographic steps and vacuum-deposition processes [4–13]. Solution-processed, high-performance semiconductors have been considered for the manufacturing of low-cost thin-film transistor (TFT) arrays/ circuits through newly developed roll-to-roll [12–26]. To date, a variety of soluble organic semiconductors have been extensively explored as potential materials with desirable electrical characteristics [17, 18, 21, 24]. However, these

---

*Corresponding author (email: lichnsa@mail.tsinghua.edu.cn)

soluble organic semiconductors still have limitations owing to their relatively inferior electronic properties, bias/environmental-stress induced instability, and process-dependent performance variation, all of which make them difficult to be employed practically. In contrast, inorganic semiconductors have been solution-processed into high performance semiconductors that have better electronic properties and stability in comparison to organic semiconductors [19, 20, 22, 23, 25–31]. In addition, much effort has been directed toward generating high-performance ZnO-based oxide semiconductors in the last decade [12,13].

Zinc oxide film can be formed by using a variety of solution processes, such as printed electronics [13, 32], nanoparticle or nanowire-based ZnO semiconducting layers based on colloidal processes [33–39], and chemical bath deposition [40–46], etc. Among the methods of solution-processed semiconductor film fabrication, the sol-gel method offers the advantages of being inexpensive and ease of the deposition [47–56]. The key to the sol-gel method involves the preparation of a stable solution for the deposition. In order to apply the sol-gel derived ZnO film for a wide range of applications with high performance, the tailoring of the crystallographic orientation and the microstructure of the film is of great importance. Li et al. developed an approach of sol-gel processed ZnO thin-film semiconductor for TFTs through thermally annealing a solution for fabricating ZnO precursor film [48–50], which demonstrated as a superior FET in TFTs with high *c*-axis orientation perpendicular to the substrate surface of polycrystalline ZnO thin-film. These studies systematically explained influence of the fabrication conditions on the FET for ZnO TFTs [50]. By optimizing the fabrication process, such as the order of concentration of precursor system in every coating cycle and the temperature of thermal annealing, etc., the prepared ZnO TFTs exhibited high FET mobility and current on/off ratio, far exceeding than those of amorphous silicon and other similar thin-film semiconductors. In this work, it was found that the FET performance of ZnO TFTs fabricated by sol-gel process was also greatly influenced by the compositions of the precursor systems which were constituted by zinc acetate, modifiers and solvents. α-Hydroxyketones and their ethanolamine derivatives are very effective modifiers for the preparation of precursor solutions for semiconductor metal oxides [57–59]; considering this, we studied the results of the sol-gel ZnO TFTs. Under similiar optimized fabrication condition, a co-modification of the mixture of acetoin and monoethanolamine for the precursor system can exhibit a high degree of crystal orientation and field-effect. The maximum mobility of 7.65 $\mathrm{cm^2V^{-1}s^{-1}}$ and current on-to-off ratio of ~10^5 – 10^6 were obtained.

2 Experimental Procedures

Precursor solutions for fabricating ZnO thin films were constituted of zinc source salt, modifiers and solvents. Zinc acetate dihydrate was employed as zinc source; Monoethanolamine, diethanolamine and the mixture of acetoin and monoethanolamine with 1:1 molar ratio were employed as modifiers; and 2-propanol and methoxyethanol were employed as solvents. Precursor solutions were prepared by dissolving zinc acetate dihydrate and modifiers with a 1:1 molar ratio in solvents. Precursor-1 solution was constituted of zinc acetate dehydrate, diethanolamine and methoxyethanol; Precursor-2 solution was constituted of zinc acetate dehydrate, diethanolamine and 2-propanol; Precursor-3 solution was constituted of zinc acetate dehydrate, monothanolamine and methoxyethanol; Precursor-4 solution was constituted of zinc acetate dehydrate, monothanolamine and 2-propanol; Precursor-5 solution was constituted of zinc acetate dehydrate, mixture of acetoin and monoethanolamine and 2-propanol. By diluting with different volumes of solvents, precursor solutions with the zinc concentration being 0.05, 0.1 and 0.25 M were prepared respectively.

The bottom-gate and top-contact device design was used in our ZnO TFTs; a typical device structure of which is shown in Figure 4(a). The ATO/ITO/glass substrate for ZnO channel, supplied by Planar Systems Inc, was structured by a glass substrate coated with a 260 nm thick layer of sputtered indium tin oxide (ITO) and a 180 nm thick layer of aluminum-titanium oxide (ATO) deposited by atomic layer deposition. ITO is a highly transparent, *n*-type conductor and served as the gate electrode. ATO, which acted as the gate dielectric, is an engineered insulator consisting of a super-lattice of alternating layers of Al_2O_3 and TiO_2. The average capacitance of the ATO layer measured was 70 nF $\mathrm{cm^{-2}}$. The channel was based on sol-gel processed ZnO thin film, of which every deposition was done by a cycle of precleaning, oxygen plasma, spin-coating, preheating and annealing: The substrate was treated with a standard acetone and isopropanol precleaning, followed by blow dry with a clean dry nitrogen gas, and subsequently, subjected to oxygen plasma. Precursor solution of a specified concentration was spin-coated atop the ATO layer with the speed of 1000 r/min for 1 min. The gel film was preheated on a hot plate at 180°C for 10 min, and then instantly annealed at a preset temperature (400°C–600°C) in ambient air for 30 min to convert the zinc precursor into ZnO. ZnO thin films were obtained by three such cycles with the zinc concentration of precursor solution in every deposition being 0.05, 0.1 and 0.25 M consecutively. To fabricate thin film transistors, 250 nm thick zinc source/drain electrodes were thermally evaporated through a shadow mask onto the ZnO film. The source/drain contact dimensions were 90 μm of length (*L*) and 600 μm of width (*W*). To make electrical contact with the ITO gate, scratches were made through to the ATO layer and zinc thin films were deposited in them by vacuum. After fabrication, the TFT devices were left for 48 hours before electrical characterization to ensure achievement of stable FET characteristics. The measurement of electrical characteristics of the TFT devices was performed with reference to our previous work [50].

The structure and characteristics of the materials were analyzed by field emission scanning electron microscopy (FE-SEM, AMRAY-1910), X-ray diffraction (XRD, Rigaku $D_{\max}$ γA X-ray diffractometer with Cu-Kα radiation, λ= 0.154178 nm) and atomic force microscopy (AFM, VEECO, Multi-Mode with Nawo-Scope IV Controller).

3 Results and Discussion

The used precursor solutions–a mixture of zinc acetate and modifiers in solvents, the modifiers used in precursor solutions acted as stabilizing agent to stabilize the formed sol and its gel film, thereby influencing the structure of the fabricated ZnO thin films. The thermogravimetric and differential thermal analyses [58–60] indicated that the crystallization and crystal growth took place largely between 400°C to 600°C during annealing processes in air. It suggested that an annealing temperature range of 400°C–600°C would be necessary for the fabrication of ZnO crystal film.

X-ray diffraction pattern (XRD) of the ZnO crystalline thin films fabricated from every precursor system is shown in Figure 1. It indicates that ZnO has a Wurtzite structure in crystalline thin films, and shows only the (002) peak at 34.4°, conclusively demonstrating a crystalline ZnO thin film with a hexagonal structure and preferred orientation of its *c*-axis being perpendicular to the substrate. 2-propanol and methoxyethanol both have barely any effect on the peak intensity. However, XRD traces of ZnO semiconductor thin films display a progressive increase in (002) peak intensity with increasing annealing temperatures. For the ZnO thin-films fabricated from precursor-3 and precursor-4 system, the (002) peak intensity gradually increases from annealing temperature of 400°C to 600°C. Similarly, for the ZnO thin films from precursor-1 and precursor-2 system, the (002) peak intensity increases slowly with the annealing temperatures of 500°C to 600°C. For the ZnO thin film from precursor-5 solution, with the co-modifier of acetoin and monoethanolamine, distinct increase is exhibited with the increasing annealing temperature and the strongest intensity is displayed at the annealing temperature of 600°C compared to other samples. The SEM images of the ZnO crystalline films from precursor-5 system, as shown in Figures 2(a)–(d), demonstrates that the sizes of ZnO particles are obviously expanding at the annealing temperature ranging from 400°C to 600°C. In comparison, the particle sizes of ZnO films from precursor systems modified with monoethanolamine or diethanolamine alone weakly increased from the annealing temperature of 500°C to 600°C (not shown here). Annealed at 600°C, the size of ZnO crystalline particles fabricated with precursor-5 system was about 50–80 nm, larger than those with the precursor systems containing only monoethanolamine or diethanolamine, as shown in Figure 2, which were general below 50 nm. This is in consistence to the XRD results. ZnO crystalline films fabricated from precursor systems with the modified monoethanolamine demonstrate some plicate structure on surface, as shown in Figures 2(g) and (h). By comparing Figures 2(e) and (f), Figures 2(g) and (h) respectively, it can be demonstrated that the role of the solvent was insignificant for the particle sizes and the surface structure.

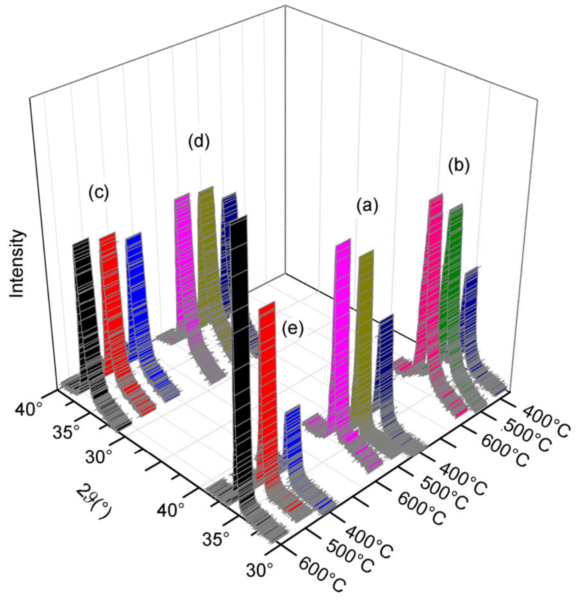

Figure 1 XRD patterns of ZnO thin films on ATO/ITO/glass fabricated from precursor-1 solution (a), precursor-2 solution (b), precursor-3 solution (c), precursor-4 solution (d) and precursor-5 solution (e), respectively; and by using the annealing temperature (T_a) of 400°C, 500°C and 600°C, respectively.

The preferred crystal orientation during the annealing process could be determined by several factors. The gel film was expected to decompose first from an atmosphere-film interface due to the compositional gradient. The initial ZnO crystal nuclei were formed and oriented at the interface during the pre-heating stage. While heated instantly up to a pre-set high temperature, the gel films experienced higher heating rates. The vaporization, decomposition and crystallization of gel films occurred within a short period. The ZnO crystalline nuclei grew larger by consuming amorphous ZnO during annealing, and the rapid heating gave the film less opportunity to relax structurally, resulting in an oriented texture. By contrary, if the heating rate was low, the gel film had enough time before crystallization; thereby resulting in randomly oriented crystals [50]. In addition, there was large volume contraction during the change from sol to gel with the successive decomposition of gel caused tensile stress parallel to the substrate surface. This stress might be helpful for the formation of the oriented structure [58, 61]. The plicated structure of the ZnO films involving modified monoethanolamine might be due to its low decomposition temperature [59]. Once the ZnO crystal is formed on the surface of the coated film at a relatively low

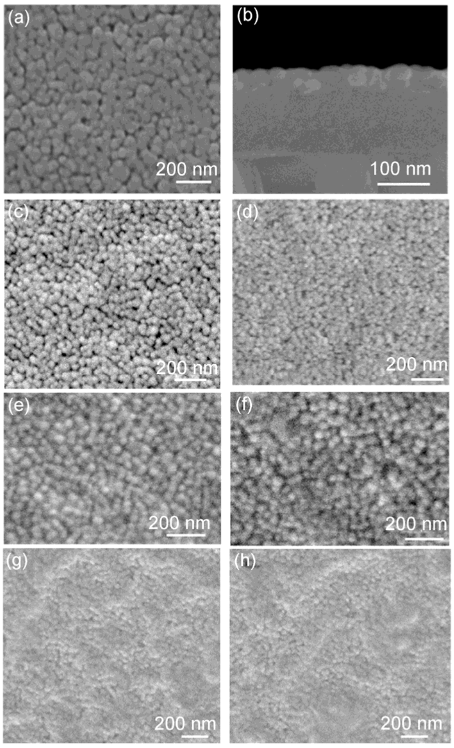

Figure 2 SEM images of ZnO semiconductor thin films deposited on ATO/ITO/glass. (a) From precursor-5, T_a: 600°C; (b) cross-section of ZnO thin film, from precursor-5, T_a: 600°C; (c) from precursor-5, T_a: 500°C; (d) from precursor-5, T_a: 400°C; (e) from precursor-1 solution, T_a: 600°C; (f) from precursor-2, T_a: 600°C; (g) from precursor-3, T_a: 600 °C; (h) from precursor-4, T_a: 600 °C.

temperature, the fluidic interior of the film could cluster under capillary force to form the plicated structure. Moreover, the decomposition of monoethanolamine at a low temperature was strictly along with the growth of ZnO crystal growth, which diminished the effect of a higher temperature on the crystalline structure of ZnO films. The crystal growth might mainly be completed at a lower temperature; while the crystal structure was hardly changed at higher temperature. Therefore the XRD peak intensity and grain sizes of ZnO crystalline films from monoethanolamine modified precursor system gradually increased with increasing temperature. In ease of the precursor system modified with diethanolamine; considering that the crystallization and crystal growth basically completed below 500°C [48], the fabricated ZnO crystalline films also demonstrated weak increase in XRD peak intensity and grain sizes at the annealing temperature of 500°C to 600°C. For the precursor system co-modified with monoethanolamine and acetoin, the reaction of monoethanolamine and acetoin generated imine and resulted in a higher decomposition temperature of the gel [56, 58], alongwith the crystallization process and crystal growth that can also be well processed at a higher temperature. Therefore, the ZnO crystalline film from precursor-5 system displayed noticeably increased (002) peak of XRD and grain sizes as the annealing temperature was increased, much larger than those from the precursor systems with a single modifier annealed at 600 °C.

Figure 3 shows the AFM topographic images of the surfaces of the ZnO films from each precursor system after annealing at 600°C. The difference in height along the surface of the ZnO film from precursor-5 system, as shown in Figure 3(e), was smaller compared to other samples, indicating its surface had the lowest roughness due to the expanding crystalline grains, which enhanced the density of the crystalline film, decreased the porosity and made highly uniform distribution of crystalline particles. The plicated structure of the surfaces of ZnO films from monoethanolamine modified precursor systems led to a high surface roughness with huge height differences along the surface of the ZnO films, as shown in Figures 3 (c) and (d). By comparing Figures 3 (a) and (b), Figures 3 (c) and (d) respectively, it was evident that the solvents had little contribution to the roughness of ZnO films. Experimental results demonstrated that the crystal structure of ZnO films was weakly influenced by the solvents. The preheating stage is a key reason in which the solvent was evaporated and a dense gel film was formed before annealing treatments. The temperature of preheating (180°C) was higher than the boiling points of the solvents and lower than the temperatures of decomposition and crystallization of the gel films, thus the newly formed gel films could have similar properties after the evaporation of the different solvents.

In Figure 2 (b), a SEM of cross-section of ZnO thin film fabricated from precursor-5 system at annealing temperature of 600°C indicates that the ZnO film was densely coated on ATO/ITO/glass substrate with a thickness of about 45 nm, which was adequate for exploiting the device performance. The other samples also possessed a similar level of the thicknesses of ZnO film. Bottom-gate, top-contact TFTs were constructed on a ATO/ITO/glass substrate using ATO, ITO, and vacuum deposited thin-film Zn metal, respectively, as gate dielectric, gate electrode, and source/drain electrodes (Figure 4 (a)). The measured FET activity of ZnO TFTs with sol-gel ZnO channels from each precursor system by using the annealing temperature of 600°C is shown in Figure 4 (b). The output curves exhibit clear pinch-off and current saturation indicating that the operation of the TFT devices conformed to standard FET theory and the Fermi level in the channel was effectively controlled by the gate bias [62]. The TFT is operated as an n-channel enhancement mode device, as evident from the fact that little drain current occurred at a gate bias of 0 V. A positive gate bias was required to generate carriers, thereby a conducting channel was induced and the channel conductivity was increased with increasing positive gate bias [4, 62]. In ZnO crystalline, excess of interstitial Zn ions or oxygen vacancies can contribute free electrons for electrical conduction [63]. Increasing the gate voltage raised the number of accumulated charges available in the channel to fill localized traps. As the traps became filled, additional charges might

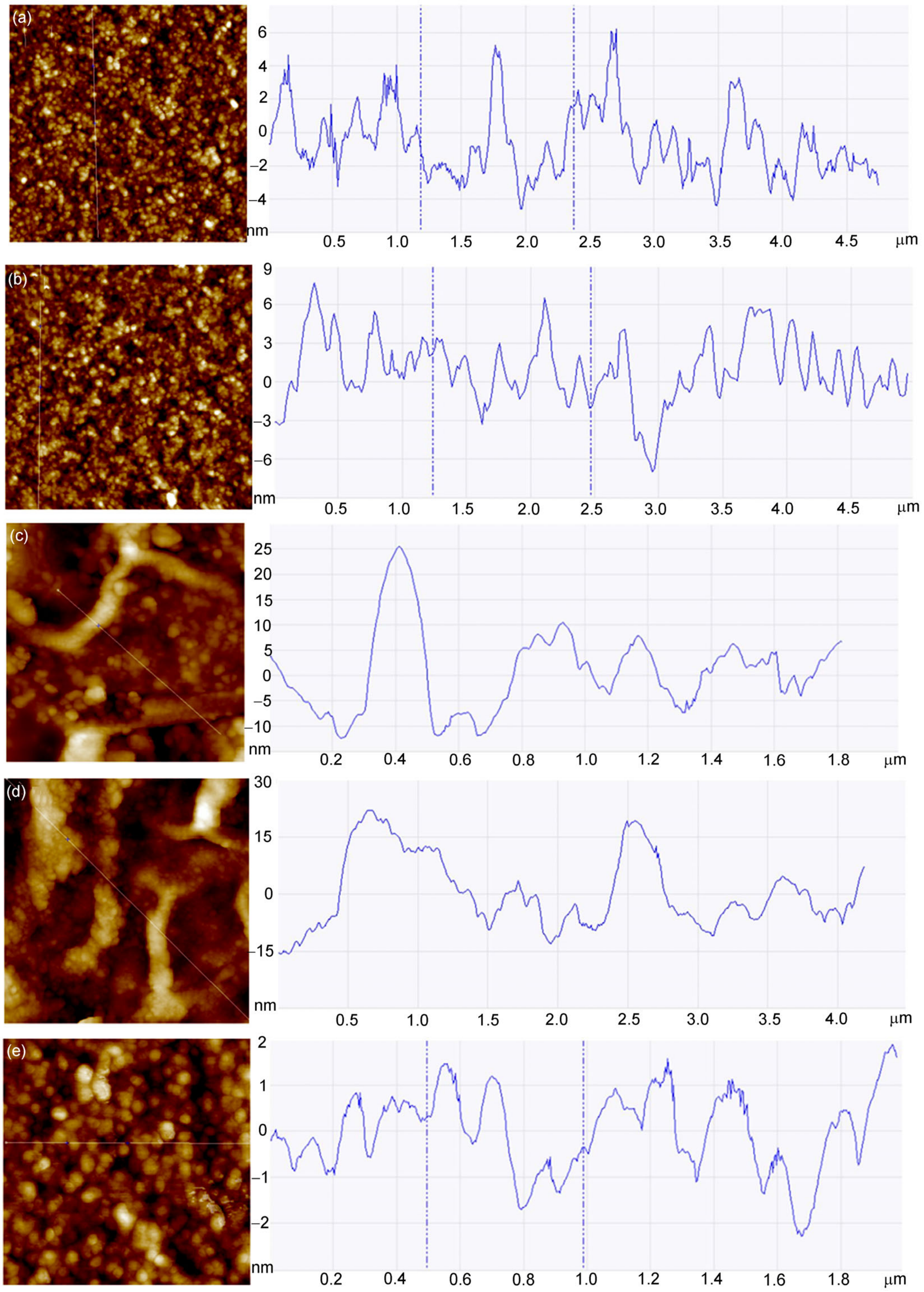

Figure 3 AFM topography images and typical line scans of ZnO samples prepared from all precursor solution after annealing at 600°C. (a) From precursor-1; (b) from precursor-2; (c) from precursor-3; (d) from precursor-4; (e) from precursor-5.

be transported with the intrinsic mobility of the delocalized semiconductor bands [4]. The mobility values extracted from the measured electrical characteristic plots can be compared with the previous work [4, 62,64].

It is believed that for efficient charge transport in TFTs along the semiconductor channel length, the most favorable ZnO crystal orientation would be one with its (002) plane parallel to or its *c*-axis perpendicular to the substrate for reason that the charge carriers are apt to transport along the paths parallel to the channel length [50, 65], while the randomly oriented crystalline in ZnO channel would result in low FET properties [50]. Experiments also indicated that

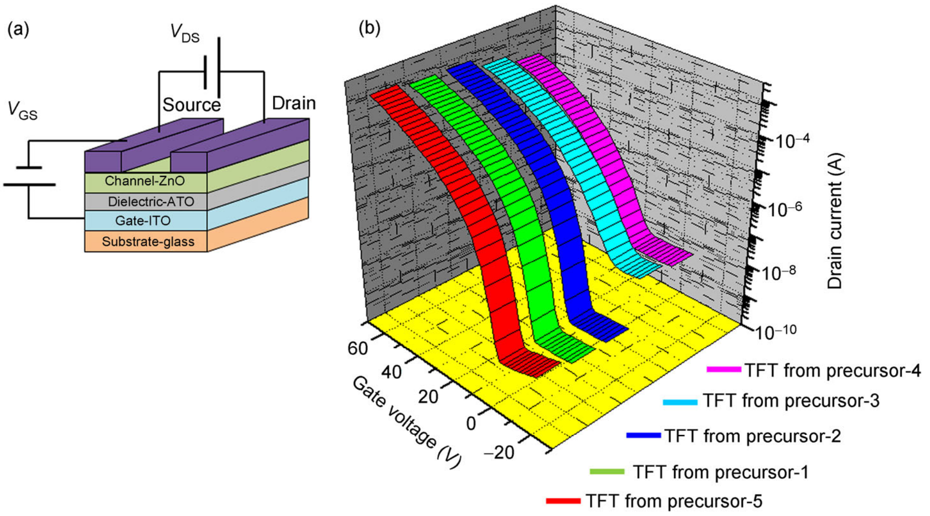

Figure 4 (a) Schematic structure of the TFT device; (b) the plots of drain current, I_{DS}, versus gate voltage, V_{GS}, at constant drain voltage, V_{DS} = 50 V, of the ZnO TFTs fabricated from every precursor system by using the annealing temperature of 600 °C.

the FET activities of the TFTs with sol-gel ZnO channels were improved as the annealing temperature was increased, reflecting that the expanding crystalline grains and higher extent of crystal orientation in ZnO channels enhanced the FET performances due to the reduction of Schottky barrier, the trapping and scattering of charge carriers and promoting transportation of charge carriers [4, 66]. Moreover, our work demonstrated that the optimum sol-gel ZnO film could be obtained by multi-deposition with the precursor solutions where their concentration would increase step by step and this was apt to form a higher density of the crystalline film with superior FET activities for ZnO TFTs [50]. Experiment results indicated that every precursor solutions could be used in order to obtain maximum FET activities of ZnO TFTs with a low process cost. Incidentally, ZnO thin films should be fabricated by deposition with the zinc concentration of precursor solution thrice and every deposition being 0.05 , 0.1 and 0.25 M in turn. This optimal concentration order is consistent to the results of our previous work [50]. The ZnO TFT with sol-gel ZnO channel from precursor-5 system annealed at 600°C demonstrated the best FET performance, which could be attributed to its strongest (002) peak of XRD (Figure 1), the largest grain sizes (Figure 2) and the flattest surface (Figure 3). It is the most regular crystal-plane orientation to let the charge carriers effectively transport along the paths parallel to the channel length with the lowest resistance and carrier scattering. Large grain sizes increased the density of the crystalline film and decreased the boundaries between the grains or domains, thus, dropping the Schottky barrier, and diminishing the trapping and scattering of charge carriers in these areas. Flat surface reduces the trapping and scattering of charge carriers in channel–dielectric interfaces and promotes transportation of the charge carriers. The extracted saturation mobility and current on-to-off ratio from the transfer plot (Figure 4 (b)) at drain voltage (V_{DS}) of 50 V and gate voltages (V_G) of -20 to 60 V for this TFT device were 7.65 cm^2 V^{-1} s^{-1} and 7.33 × 10^5, respectively. The extracted saturation mobility of ZnO TFT devices fabricated from precursor-1 and precursor-2 systems was 5.18 and 5.24 cm^2 V^{-1} s^{-1}, respectively. Their current on-to-off ratios were also ~10^5–10^6. The ZnO TFTs fabricated from precursor-3 and precursor-4 system which were modified by monoethanolamine demonstrated relative low FET performances, their extracted saturation mobilities them were 1.75 and 1.88 cm^2 V^{-1}s^{-1}, respectively. Their current on-to-off ratios were ~10^4–10^5, which were considerably inferior. The reason was due to their plicated structure on surface, as shown in Figures 2 (f) and (g), which would increase the trapping and the scattering while drop the transport efficiency of the charge carriers during the transport process. Moreover, this plicated structure in surface also increases the interfacial contact resistance between semiconductor channel and electrode materials, resulting in an inferior FET performance. The experiment results shown in Figure 4 also indicates that the role of the solvent was of little significance for the FET performances of ZnO TFTs due to its limited influence on the crystal structure of the sol-gel ZnO films.

Through the measurement of optical absorbance spectrum, the optical transmittance of all the ZnO TFTs was above 80% in the spectral range of visible light, which is an advantage in electronic driver for displays.

4 Conclusions

Transparent conductive oxides are promising candidates for manufacturing transparent electronics for display applications. The use of solution-processing techniques allows a dramatic reduction in cost per unit area of electronic functionality. By optimizing the deposition processes, it is possible to construct the solution-processed transparent semiconductor films that offer enhanced performance comparable to those fabricated by physical methods, in addition to being economical.

In this work, we prepared stable and highly mobile ZnO thin-film transistors through sol-gel process. Monoethanolamine, diethanolamine and the mixture of acetoin and monoethanolamine were examined as sol-gel modifiers for a preparation of ZnO TFTs. When the modified sol was used in the ZnO film preparation by rapid heating, *c*-axis orientated ZnO grains were crystallized. The extent of the crystal orientation, grain sizes and the surface flatness of the resultant ZnO film from the sol co-modified with acetoin and monoethanolamine were greater than those of the films from the sol modified by monoethanolamine or diethanolamine alone. Results of optimization of fabrication conditions have shown that, TFTs incorporating sol-gel ZnO channel semiconductors possess excellent FET characteristics. TFT with ZnO channel fabricated from the co-modified sol by acetoin and monoethanolamine with the annealing temperature as 600°C exhibited the highest field-effect performance, the maximum mobility of 7.65 $\text{cm}^2\text{V}^{-1}\text{s}^{-1}$ and the current on-to-off ratio of ~10^5–10^6. The excellent FET characteristics of the sol-gel ZnO TFTs are appropriate enough for enhancing the brightness and resolution of active matrix organic light-emitting diodes and is applicable for the switching devices in active-matrix flat-panel displays [67,68]. The performance was largely endurable, highly consistent and reproducible with little transistor-to-transistor variation.

This work was supported by the Major State Basic Research Development Program of China (Grant No.10332020).

1 Schroder D K. Semiconductor Material and Device Characterization. New York: Wiley, 1998

2 Yang A L, Yang Y, Zhang Z Z, et al. Photoluminescence and defect evolution of nano-ZnO thin films at low temperature annealing. Sci China Tech Sci, 2013, 56: 25–31

3 Li X, Jiang Y D, Tai H L, et al. The fabrication and optimization of OTFT formaldehyde sensors based on Poly(3-hexythiophene)/ZnO composite films. Sci China Tech Sci, 2013, 56: 1877–1882

4 Howard W E. Thin Film Transistors. New York: Dekker, 2003

5 Cui J B, Soo Y C, Kandel H, et al. Investigations of ZnO thin films deposited by a reactive pulsed laser ablation. Sci China Ser E-Tech Sci, 2009, 52: 99–103

6 Zhao L, Xu C S, Liu Y X, et al. Effects of temperature and pressure on the structural and optical properties of ZnO films grown by pulsed laser deposition. Sci China Tech Sci, 2010, 53: 317–321

7 Su G, Song M Q, Sun W Z, et al. Electrodeposition in organic system and properties of NiO electrochromic films. Sci China Tech Sci, 2012, 55: 1545–1550

8 Chen Y Y, Chen S G, Chen Y, et al. Surface analysis and electrochemical behaviour of the self-assembled polydopamine/dodecanethiol complex films in protecting 304 stainless steel. Sci China Tech Sci, 2012, 55: 1527–1534

9 Wang L H, Shu Y H, Fan J. Effect of humidity on microstructure and properties of YBCO films prepared by Electron Beam Coevaporation. Sci China Tech Sci, 2012, 55: 2291–2294

10 Lei J X, Ma F Z, Shi Y, et al. Synthesis of polycrystalline gamma-AlON powders by novel wet chemical processing. Sci China Tech Sci, 2012, 55: 3405–3410

11 Bu X B, Wang L B, Li H S, et al. Preparation of composite adsorbent of sawdust and $CaCl_2$ by carbonization method for creating pore. Sci China Tech Sci, 2012, 55: 2404–2408

12 Frenzel H, Lajn A, Wenckstern H V, et al. Recent progress on ZnO-based metal-semiconductor field-effect transistors and their application in transparent integrated circuits. Adv Mater, 2010, 22: 5332–5349

13 Fortunato E, Barquinha P, Martins R. Oxide semiconductor thin-film transistors: a review of recent advances. Adv Mater, 2012, 24: 2945–2986

14 Obrien P, Saeed T, Knowlcs J. Speciation and the nature of ZnO thin films from chemical bath deposition. J Mater Chem, 1996, 6: 1135–1139

15 Ohyama M, Kozuka H, Yoko T. Sol-gel preparation of ZnO films with extremely preferred orientation along (002) plane from zinc acetate solution. Thin Solid Films, 1997, 306: 78–85

16 Yamabi S, Imai H. Growth conditions for wurtzite zinc oxide films in aqueous solutions. J Mater Chem, 2002, 12: 3773–3778

17 Sirringhaus H. Device physics of solution-processed organic field-effect transistors. Adv Mater, 2005, 17: 2411–2425

18 Klauk H. Organic Electronics: Materials, Manufacturing, and Applications. Weinheim: Wiley-VCH, 2006

19 Subramanian V, Bakhishev T, Redinger D. Solution-processed zinc oxide transistors for low-cost electronics applications. J Display Technol, 2009, 5: 525–530

20 Han S Y, Lee D H, Herman G S, et al. Inkjet-printed high mobility transparent–oxide semiconductors. J Display Technol, 2009, 5: 520–524

21 Wang H, Ji Z Y, Liu M, et al. Advances in organic field-effect transistors and integrated circuits. Sci China Ser E-Tech Sci, 2009, 52: 3105– 3116

22 Ryu M K, Park K B, Seon J B, et al. Solution-processed oxide semiconductors for low-cost and high-performance thin-film transistors and fabrication of organic light-emitting-diode displays. J Soc Inf Disp, 2010, 18: 734–744

23 Jeong S, Moon J. Low-temperature, solution-processed metal oxide thin film transistors. J Mater Chem, 2012, 22: 1243–1250

24 Li Y, Liu Q, Wang X Z, et al. Pentacene thin film transistor with low threshold voltage and high mobility by inserting a thin metal phthalocyanines interlayer. Sci China Tech Sci, 2012, 55: 417–420

25 Park J S, Maeng W-J, Kim H-S, et al. Review of recent developments in amorphous oxide semiconductor thin-film transistor devices. Thin Solid Films, 2012, 520: 1679–1693

26 Shimoda T, Matsuki Y, Furusawa M, et al. Solution-processed silicon films and transistors. Nature, 2006, 440: 783–786

27 Ridley B A, Nivi B, Jacobson J M. All-inorganic field effect transistors fabricated by printing. Science, 1999, 286: 746–749

28 Byrne P D, Facchetti A, Marks T J. High-performance thin-film transistors from solution-processed cadmium selenide and a self-assembled multilayer gate dielectric. Adv Mater, 2008, 20: 2319–2324

29 Mitzi D B, Copel M, Chey S J. Low-voltage transistor employing a high-mobility spin-coated chalcogenide semiconductor. Adv Mater, 2005, 17: 1285–1289

30 Mitzi D B, Copel M, Murray C E. High-mobility p-type transistor based on a spin-coated metal telluride semiconductor. Adv Mater, 2006, 18: 2448–2452

31 Mitzi D B. Solution-processed inorganic semiconductors. J Mater Chem, 2004, 14: 2355–2365

32 Subramanian V, Fréchet J M J, Chang P C, et al. Progress towards development of all-printed RFID tags: Materials, Processes, and Devices. Proc IEEE, 2005, 93: 1330–1338

33 Faber H, Burkhardt M, Jedaa A, et al. Low-temperature solution-processed memory transistors based on zinc oxide nanoparticles. Adv Mater, 2009, 21: 3099–3104

34 Schneider J J, Hoffmann R C, Engstler J, et al. Synthesis, characterization, defect chemistry, and FET properties of microwave-derived nanoscaled zinc oxide. Chem Mater, 2010, 22: 2203–2212

35 Richter T V, Stelzl F, Schulz-Gericke J, et al. Room temperature vacuum-induced ligand removal and patterning of ZnO nanoparticles: from semiconducting films towards printed electronics. J Mater Chem, 2010, 20: 874–879

36 Sun B, Sirringhaus H. Solution-processed zinc oxide field-effect transistors based on self-assembly of colloidal nanorods. Nano Lett, 2005, 5: 2408–2413

37 Huang X, Coffer J L. Emissive Er/ZnO/GeO$_x$(SiO$_2$) oxide nanofibers derived from anelectrospinning process. Cryst Growth Des, 2012, 12: 2362–2366

38 Sun B, Peterson R L, Sirringhaus H, et al. Low-temperature sintering of in-plane self-assembled ZnO nanorods for solution-processed high-performance thin film transistors. J Phys Chem C, 2007, 111: 18831–18835

39 Sun B, Sirringhaus H. Surface tension and fluid flow driven self-assembly of ordered ZnO nanorod films for high-performance field effect transistors. J Am Chem Soc, 2006, 128: 16231–16237

40 Ohya Y, Niwa T, Ban T, et al. Thin film transistor of ZnO fabricated by chemical solution deposition. Jpn J Appl Phys, 2001, 40: 297–298

41 Zhang X, Huang X, Li C, et al. Dye-sensitized solar cell with energy storage function through PVDF/ZnO nanocomposite counter electrode. Adv Mater, 2013, 25: 4093–4096

42 Li C S, Li Y N, Wu Y L, et al. ZnO field-effect transistors prepared by aqueous solution-growth ZnO crystal thin film. J Appl Phys, 2007, 102: 076101

43 Redinger D, Subramanian V. High-performance chemical-bath-deposited zinc oxide thin-film transistors. IEEE Trans Electron Devices, 2007, 54: 1301–1307

44 Sun K, Wei W, Ding Y. Crystalline ZnO thin film by hydrothermal growth. Chem Commun, 2011, 47: 7776–7778

45 Li C S, Qiao Y J, Li Y M. Decorating multiwalled carbon nanotubes with zinc oxide nano-crystallines through hydrothermal growth process. Sci China Tech Sci, 2012, 55: 1365–1370

46 Wang C X, Zhang X D, Wang D F, et al. Synthesis of nanostructural ZnO using hydrothermal method for dye-sensitized solar cells. Sci China Tech Sci, 2010, 53: 1146–1149

47 Cheng H C, Chen C F, Tsay C Y. Transparent ZnO thin film transistor fabricated by sol-gel and chemical bath deposition combination method. Appl Phys Lett, 2007, 90: 012113

48 Ong B S, Li C S, Li Y N, et al. Stable, solution-processed, high-mobility ZnO thin-film transistors. J Am Chem Soc, 2007, 129: 2750– 2751

49 Li C S, Li Y N, Wu Y L, et al. Performance improvement for solution-processed high-mobility ZnO thin-film transistors. J Phys D-Appl Phys, 2008, 41: 125102

50 Li C S, Li Y N, Wu Y L, et al. Fabrication conditions for solution-processed high-mobility ZnO thin-film transistors. J Mater Chem, 2009, 19: 1626–1634

51 Hwang Y H, Seo S-J, Bae B-S. Fabrication and characterization of sol-gel-derived zinc oxide thin-film transistor. J Mater Res, 2010, 25: 695–700

52 Tsay C-Y, Fan K-S, Wang Y-W. Transparent semiconductor zinc oxide thin films deposited on glass substrates by sol-gel process. Ceram Intern, 2010, 36: 1791–1795

53 Sengupta J, Sahoo R K, Bardhan K K. Influence of annealing temperature on the structural, topographical and optical properties of sol-gel derived ZnO thin films. Mater Lett, 2011, 65: 2572–2574

54 Tsay C-Y, Fan K-S, Chen S-H, et al. Preparation and characterization of ZnO transparent semiconductor thin films by sol–gel method. J Alloy Compd, 2010, 495: 126–130

55 Singh S, Chakrabarti P. Simulation, fabrication and characterization of sol-gel deposited ZnO based thin film transistors. Sci Technol Adv Mater, 2012, 4: 199–203

56 Takahashi Y, Ohsugi A, Arafuka T, et al. Development of new modifiers for titanium alkoxide-based sol-gel process. J Sol-Gel Sci Technol, 2000, 17: 227–238

57 Ohya T, Kabata M, Ban T, et al. Effect of α-Hydroxyketones as chelate ligands on dip-coating of zirconia thin films. J Sol-Gel Sci Technol, 2002, 25: 43–50

58 Yutaka O, Takatomo O, Takayuki B, et al. Microstructure of sol-gel ZnO thin films fabricated using ethanolamine and hydroxyketone modifiers. J Ceram Soc Japan, 2005, 113: 220–225

59 Ohyama M, Kozuka H, Ypko T, et al. Preparation of ZnO films with preferential orientation by sol-gel method. J Ceram Soc Japan, 1996, 104: 296–300

60 Ohya Y, Saiki H, Tanaka T, et al. Microstructure of TiO$_2$ and ZnO films fabricated by the sol-gel method. J Am Ceram Soc, 1996, 79: 825–830

61 Kozuka H, Takenaka S, Tokita H, et al. Stress and cracks in gel-derived ceramic coatings and thick film formation. J Sol-Gel Sci Technol, 2003, 26: 681–686

62 Horowitz G. Organic thin film transistors: from theory to real devices. J Mater Res, 2004, 19: 1946–1962

63 Carcia P F, Mclean R S, Reilly M H, et al. Transparent ZnO thin-film transistor fabricated by rf magnetron sputtering. Appl Phys Lett, 2003, 82: 1117–1119

64 Barquinha P, Pimentel A, Marques A, et al. Influence of the semiconductor thickness on the electrical properties of transparent TFTs based on indium zinc oxide. J Non-Cryst Solids, 2006, 352: 1749–1752

65 Fortunato E, Barquinha P, Pimentel A, et al. Recent advances in ZnO transparent thin film transistors. Thin Solid Films, 2005, 487: 205–211

66 Hossain F M, Nishii J, Takagi S, et al. Modeling of grain boundary barrier modulation in ZnO invisible thin film transistors. Physica E, 2004, 21: 911–915

67 Kumar A, Nathan A, Jabbour G E. Does TFT mobility impact pixel size in AMOLED backplanes? IEEE Trans Electron Devices, 2005, 52: 2386–2394

68 Tang M, Guo Y Q, Yuan J, et al. Review of some recent progress on materials science researches in China. Sci China Chem, 2012, 55: 2497–2502